Guglielmi, S. *et al.* (2024). *Géotechnique* **74**, No. 13, 1881–1885 [https://doi.org/10.1680/jgeot.22.D.006]

DISCUSSION

Analysis of the micro to macro response of clays to compression

SIMONA GUGLIELMI*, FEDERICA COTECCHIA†, FRANCESCO CAFARO‡, ANTONIO GENS§, SERGE LEROUEIL||, DAVID W. HIGHT¶ and JACQUES LOCAT||

Contribution by Serge Leroueil, David W. Hight and Jacques Locat

The writers congratulate the authors for having done such a thorough overview of the information concerning the evolution of the microfabric of clayey soils, reconstituted or natural, soft or stiff, and having developed a general conceptual model that is summarised in their Fig. 22 (Guglielmi *et al.*, 2022). The model refers to clays that are not influenced by a significant amount of organic matter, carbonates (e.g. Soccodato, 2003) or diatoms (e.g. Locat & Tanaka, 2001). The writers agree with this model and here present some comments rather than a discussion as such.

The model is described in a void index (I_v) plotted against log σ'_v diagram, as shown in Fig. 22 and in the left part of Fig. 23. However, if the void index is used by some researchers, it is rarely used in geotechnical practice, and it may be convenient to consider an equivalent parameter that is the liquidity index (I_L). As the reference compression curve (ICL) depends on sample preparation, temperature, water salinity and rate of loading, the former (I_v) is probably not more 'intrinsic' or fundamental than the second (I_L), even if it is an interesting reference. An approximate liquidity index scale is drawn on the right side of Fig. 23. As indicated, a liquidity index of 1·0 ($w = w_L$) would correspond to a void index of about 1·2 while a liquidity index of 0 ($w = w_p$) would correspond to a void index of about −0·8.

The last column of Fig. 23 schematically shows the evolution of the pore size distribution (PSD) with compression, as described by the authors. If the PSD of a soft clay is bimodal (Fig. 23(a)), compression progressively closes the inter-aggregate pores without significantly changing the total volume and the size of the intra-aggregate pores (Fig. 23(b)). From experience with clays from eastern Canada (Delage & Lefebvre, 1984; Lapierre *et al.*, 1990; Locat, 1995), the aggregates forming the soft clays are at a water content close to the plastic limit of the soil. It is when the inter-aggregate pores are essentially closed (Fig. 23(c)) that the size and the total volume of the intra-aggregate pores decrease (Fig. 23(d)). This concept is illustrated by Locat (1995) using the porosity index ($I_n = (w - w_p)/w_p$) so that when $I_n = 0$, the water content is at the plastic limit and the inter-aggregate pores are essentially closed.

The central column of Fig. 23 shows the index of fabric orientation that increases with clay one-dimensional (1D) compression, as described in the paper. An implication is an increase of permeability anisotropy with clay compression. This was shown by Al-Tabbaa & Wood (1987) on kaolin and by Leroueil *et al.* (1990) and others on natural clays. As shown in Fig. 24, if $r_k = k_h/k_v$ is close to 1·1 for soft marine clays with I_L values larger than about 0·9 (Leroueil *et al.*, 1990), it increases at lower I_L to reach values from 1·5 to 3 at a liquidity index of zero.

Probably one important aspect that could be added to the authors' soil fabric model is the effect of soil deposition in an environment with limited bioturbation, which may give rise to surfaces of lower strength (bedding). Leblond (personal communication, 2002; see Leroueil *et al.* (2003)) performed undrained torsional shear hollow cylinder tests on Louiseville clay, Quebec, at a depth close to that of the samples tested by Lapierre *et al.* (1990). The natural clay tested had a liquidity index of 1·1, a vertical yield stress σ'_{vy} of 180 kPa and was consolidated under an isotropic effective stress equal to $0{\cdot}3\sigma'_{vy}$ before shearing with the axis of the major principal stress axis at an angle β to the vertical that varied from 0° (conventional compression) to 75°. Other tests were performed at β angles of 0°, 22° and 29° after isotropic consolidation to 0·19, 0·44 and $0{\cdot}54\sigma'_{vy}$. Well-defined failure surfaces were observed in all tests, and the angles of these surfaces to the horizontal, θ, are plotted as a function of β in Fig. 25(a). It can be seen that, for β angles up to about 25°, they follow the theoretical Mohr–Coulomb relationship (dashed line) and that, for larger β angles, failure always occurred on horizontal planes ($\theta = 0°$), at variance with Mohr–Coulomb and providing evidence for the effect of bedding.

All the tests performed at β values of 0°, 22° and 29° gave the strength envelopes shown in Fig. 25(b), corresponding to $\phi' = 28°$ and c' about equal to $0{\cdot}2\sigma'_{vy}$. For β values larger than 30°, Leblond (personal communication, 2002) calculated the stress conditions at failure on the horizontal plane and found the results shown on Fig. 25(b). As can be seen, the strength on horizontal planes (bedding planes) is significantly smaller than that along other planes. A partial explanation may come from the observation (at least for clays from eastern Canada; e.g. Lapierre *et al.* (1990)) that the observed roughness along horizontal planes is smaller than along vertical planes. More generally, it may come from the slow deposition process and the smoothing of the sea bottom by water currents and animals.

It is also worth noting that undrained torsional shear hollow cylinder tests performed by Brosse (2012) on Oxford clay

Manuscript received 22 March 2023; revised manuscript accepted 22 March 2023. First published online ahead of print 5 April 2023.
* Scuola Superiore Meridionale, Università degli Studi di Napoli Federico II, Napoli, Italy (Orcid:0000-0003-0416-6836).
† Department of Civil, Environmental, Land, Building Engineering and Chemistry, Politecnico di Bari, Bari, Italy (Orcid:0000-0001-9846-4193).
‡ Department of Civil, Environmental, Land, Building Engineering and Chemistry, Politecnico di Bari, Bari, Italy (Orcid:0000-0001-5076-8606).
§ Departamento de Ingeniería Civil y Ambiental, Universitat Politécnica de Catalunya, Barcelona, Spain (Orcid:0000-0001-7588-7054).
|| Laval University, Québec, Canada.
¶ Geotechnical Consulting Group, London, UK.

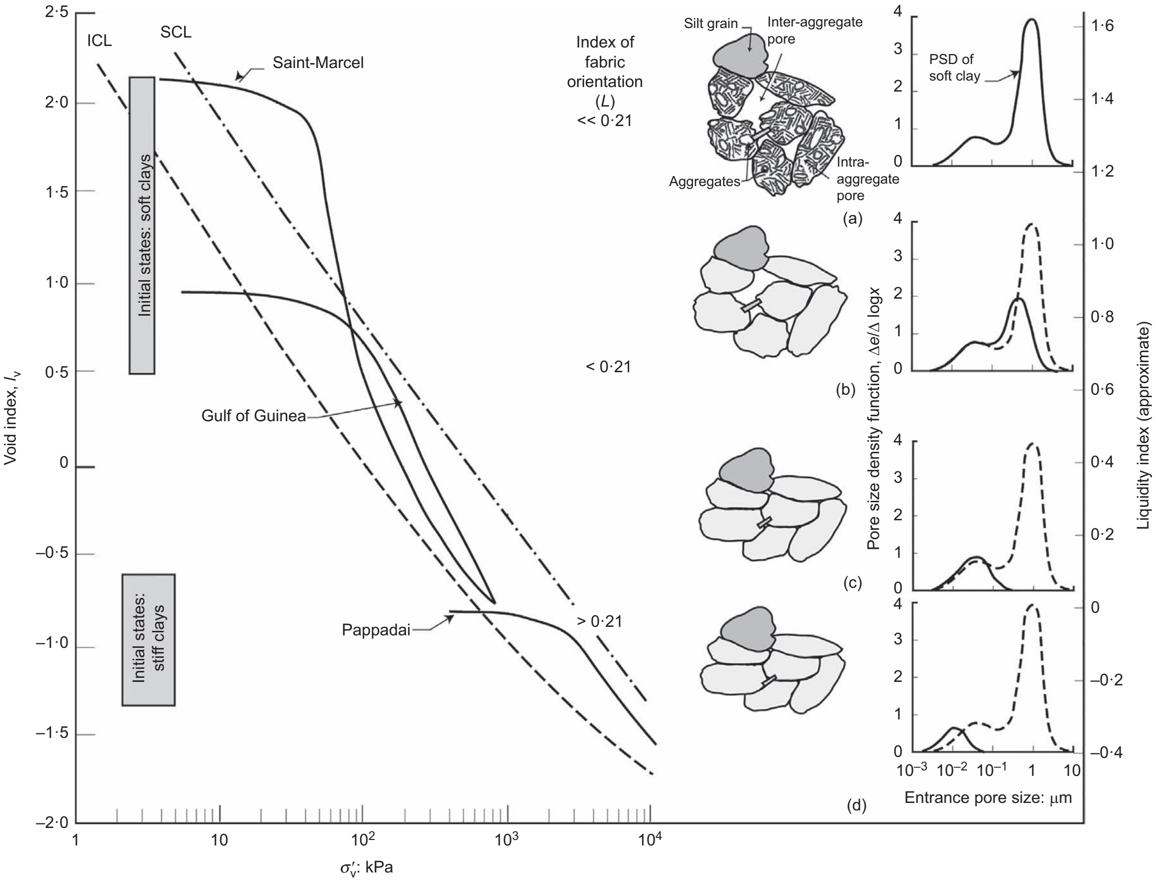

Fig. 23. Evolution of the fabric of clayey soils under 1D compression. Far left column: compression lines in an I_v plotted against log σ'_v diagram (after Guglielmi *et al.*, 2022); an approximate I_L scale is plotted on the right side of the figure; second left column: index of fabric orientation, *L* (from Guglielmi *et al.* (2022)). Third left column: schematic representation of the fabric. Far right column: schematic diagrams of pore size distribution (PSD)

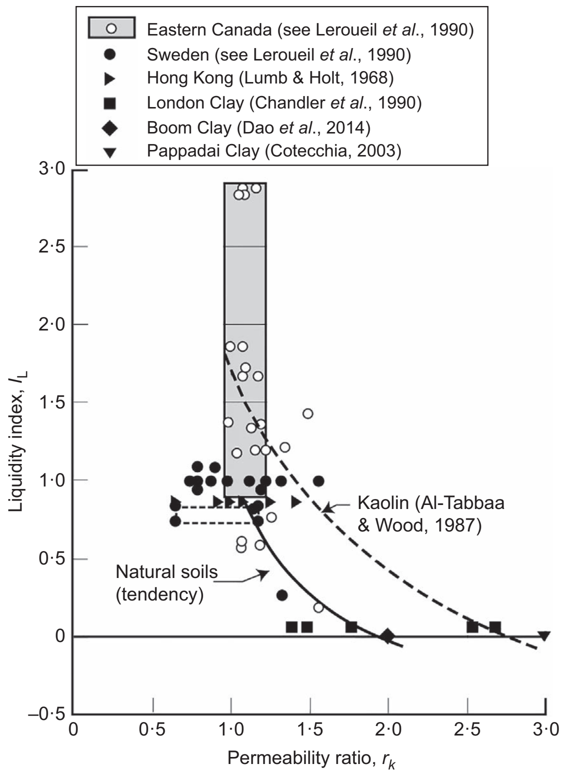

Fig. 24. Permeability ratio r_k as a function of the liquidity index I_L for clayey soils (modified after Leroueil *et al.* (1990))

($I_L = -0{\cdot}25$) (Fig. 26) show a behaviour similar to that observed on Louiseville clay (Fig. 25(a)). Brosse *et al.* (2017) describe Oxford clay as having a strong orientation of particles and shells, which probably explains the observed shear behaviour. In any case, bedding is certainly a factor that could complement the authors' general model for natural soft to stiff clayey soils. When existing, it acts as a series of discontinuities complicating the mechanical behaviour of soils. Obviously, in hard and stiff clays, the effects of bedding can be overridden by the presence of fissures that often have preferred orientation other than horizontal.

Authors' reply

The authors wish to thank the discussion contributors for their appreciations of their research, as presented in the recent paper (Guglielmi *et al.*, 2022), on the evolution of microstructure at different stages of compression of a number of multi-mineral clays, both reconstituted and natural, ranging from soft to stiff. The authors are also grateful to the discussion contributors for sharing their comments and adding interesting considerations to complement the conceptual model resulting from the analysis, summarised in Fig. 22 in the void index (I_v) against σ'_v plot.

The authors essentially agree with the discussion contributors' comments and would like to add further remarks, which will be reported following the discussion outline.

First, the discussers point out that the model could be conveniently presented in a liquidity index (I_L) plotted

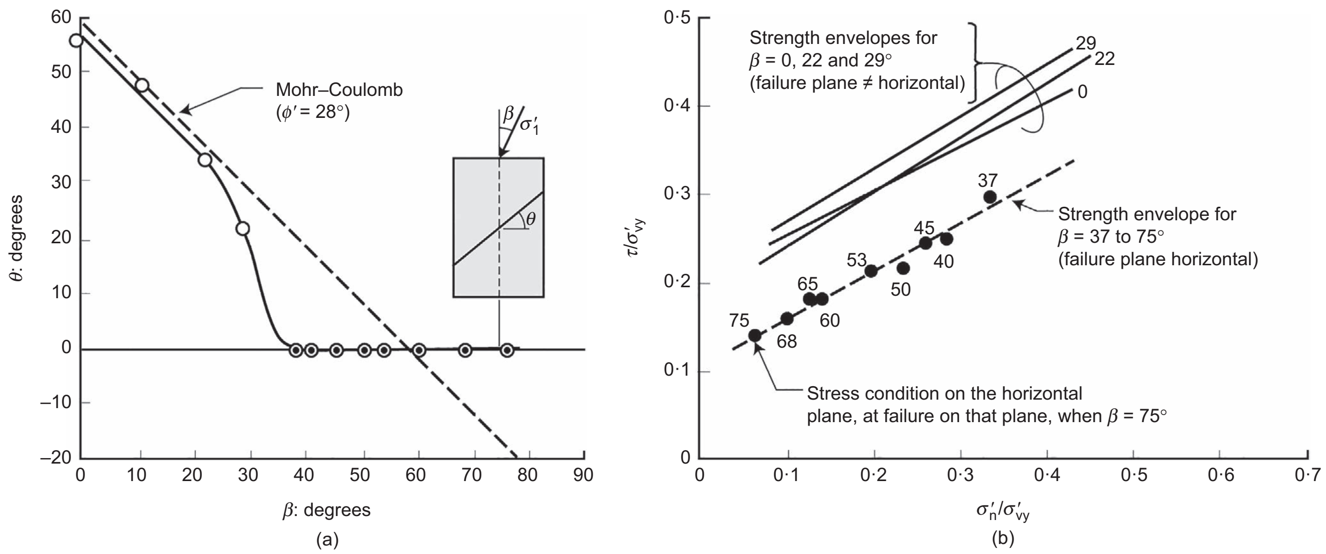

Fig. 25. Undrained tests performed on Louiseville clay in a torsional shear hollow cylinder: (a) inclination of failure plane with the horizontal, θ, plotted against the angle of major principal stress axis rotation, β, for an isotropic consolidation effective stress equal to $0{\cdot}3\sigma'_{vy}$; (b) strength envelopes obtained for different β values (after Leblond, personal communication, 2002 and Leroueil *et al.* (2003))

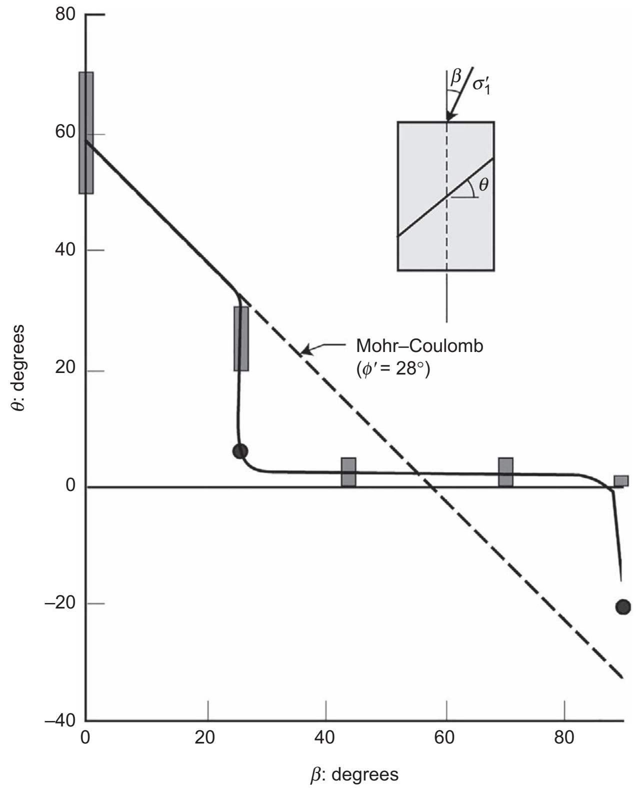

Fig. 26. Undrained tests performed on Oxford clay in a torsional shear hollow cylinder. Inclination of failure plane with the horizontal, θ, plotted against the angle of major principal stress axis rotation, β (after Brosse (2012))

against σ'_v diagram, as the liquidity index is as basic as the void index, I_v, but far more common in geotechnical practice. The authors agree and hence present a new version of Fig. 22 (Fig. 27) in accordance with the discussers' suggestion, which is greatly appreciated.

The compressibility curves of most of the soft and stiff clays analysed in the paper are replotted in the I_L against σ'_v diagram, using the properties of the clays reported in Table 1 by Guglielmi *et al.* (2022) and in the literature referenced. The intrinsic compression lines (ICLs) of Gulf of Guinea (GoG) clay and Pappadai clay are reported as dashed lines, namely ICL_{GoG} and ICL_{Pa}, respectively. It is interesting to remark that the two lines plot close together but do not overlap, as expected following Skempton & Northey (1952) and Skempton (1969), who detected the non-uniqueness of the intrinsic compression curves in the I_L against σ'_v plot.

The microstructural states for the two reconstituted clays (GoG1*, GoG2* and GoG3* and Pa1*, the labels are not shown for clarity; see Guglielmi *et al.* (2022)) are reported along ICL_{GoG} and ICL_{Pa}, and those of the remaining clays are shown to plot between or close to the two mentioned ICLs.

As suggested by the discussers in their Fig. 23, the central and last columns of Fig. 27 show the re-organisation of the micro-fabric and its degree of orientation, *L*, and the schematic evolution of the PSD with the clay 1D compression.

Analysing the data in terms of I_L plotted against σ'_v shows that most of the conversion of the clay micro-fabric features from honeycomb-like (Griffiths & Joshi, 1990) to well oriented (evolution of Sfondrini (1975); see Figure 7 in Guglielmi *et al.* (2022)) occurs when the clay has achieved a plastic consistency, in particular during the compression bringing the clay from $I_L = 1$ to I_L of about 0·3–0·4.

As stated by the discussers, inspection of the PSD of natural and remoulded Louiseville clay at different stages of 1D compression (Locat, 1995) has shown that the closure of the inter-aggregate pore space, resulting in a monomodal PSD, is attained in specimens at a water content close to the plastic limit. This suggests that maximum compression of the inter-aggregate pore space is achieved by a water content close to the plastic limit (Locat, 1995). Microstructural analyses on stiff Pappadai and Lucera clay, as well as other results from the literature shown in the paper, confirm that clays at $I_L = 0$ ($w = w_P$; Fig. 27) exhibit a monomodal PSD of prevailing intra-aggregate pore volume.

The authors thank the discussers for adding this alternative view to their framework.

A second point raised by the discussers in their discussion is the increase in permeability anisotropy with clay compression, associated with the observed increase in fabric orientation. This is seen to apply to both

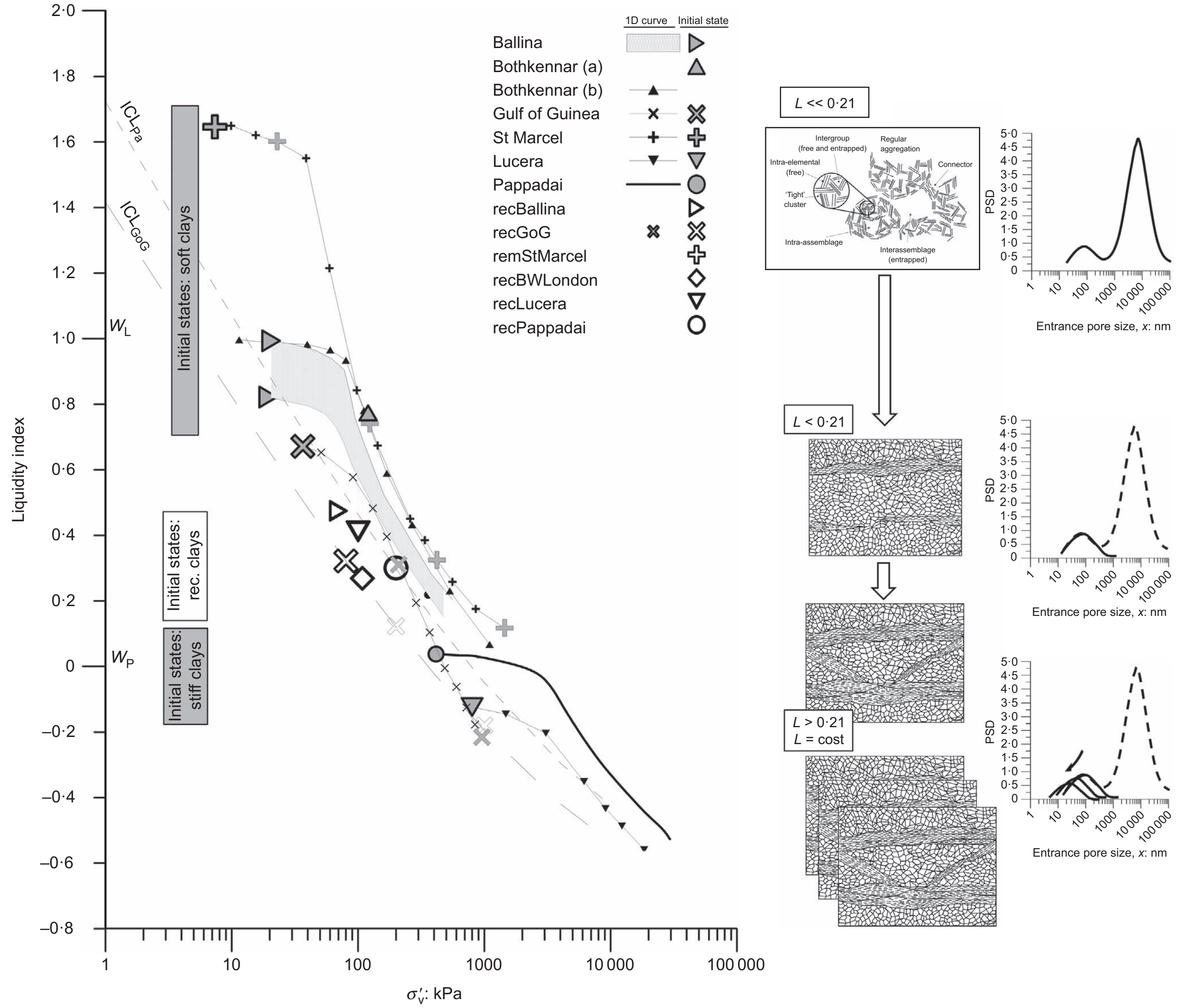

Fig. 27. Conceptual model of the microstructural features of multi-mineral clays and their evolution at different stages of compression in the liquidity index (I_L) plotted against σ'_v diagram (adapted from Guglielmi *et al*. (2022) and from the discussion contribution above)

reconstituted and natural clays, as observed by the discussers and illustrated in their Fig. 24. Lollino *et al*. (2005) showed that natural Pappadai clay (I_L close to 0; see Fig. 27) has a ratio in horizontal to vertical permeability, $r_k = k_h/k_v$, of about 3, as shown by the discussers in their Fig. 24. The suggested explanation for the anisotropy ratio r_k of Pappadai clay being much higher than for other natural clays (see e.g. the experimental points for Boom or London clay, or for Sweden clay, in Fig. 24 after Leroueil *et al*. (1990)) is the presence of horizontal lamination planes originated at deposition, which are found to incorporate coarser carbonatic material (mainly nannofossils; Cotecchia & Chandler (1995) and Cotecchia (2003)). The origin of these laminations, probably due to systematic alternation of the conditions of sedimentation (e.g. O'Brien & Slatt, 1990), cannot be established in detail, but they fall within the typical heterogeneities characterising natural clays which can be responsible for the increase in permeability anisotropy with respect to the reconstituted clay.

Finally, the authors agree with the discussers that bedding could be an additional feature complementing their general model. They believe that invoking the 'roughness' as a reason for strength along failure surfaces is questionable for clays, considering that this factor more strictly pertains to geomaterial interfaces or failure surfaces within rocks and granular soils. Embracing the suggestion, the authors would generalise the observation adding to bedding any other factor of weakness for planes, both syngenetic and diagenetic, such as localised swelling due to electrokinetic phenomena. For example, Cafaro & Cotecchia (2001) observed, for a specimen of stiff clay including two portions of different colour (Fig. 28), yellow and yellow-grey, which was subjected to undrained shear after isotropic consolidation to $p' = 1000$ kPa, a shear band including the slip surface developed within the transition colour band. With equivalent carbonate contents measured at the end of the test for both portions (25·7% and 25·9%), the loss of strength along the transition colour band was hypothesised to be the effect of localised swelling at the border between a reducing environment and an oxidising one. However, since incorporating surfaces of lower strength probably diminishes the role of representative element volume (REV) of the specimen, enlarged REV sizes should be adopted in case of significant bedding, to allow anisotropy without including heterogeneity.

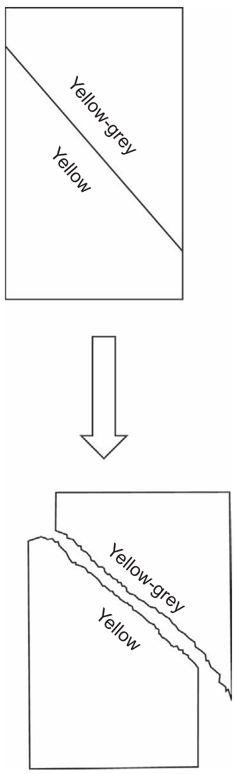

Fig. 28. Failure of a natural clay specimen formed of two portions of different oxidation degree (after Cafaro & Cotecchia (2001))

REFERENCES

Al-Tabbaa, A. & Wood, D. M. (1987). Some measurements of the permeability of kaolin. *Géotechnique* **37**, No. 4, 499–503, https://doi.org/10.1680/geot.1987.37.4.499.

Brosse, A. M. (2012). *Study of the anisotropy of British stiff clays using a hollow cylinder apparatus*. PhD thesis, Imperial College London, London, UK.

Brosse, A. M., Jardine, R. J. & Nishimura, S. (2017). The undrained shear strength anisotropy of four Jurassic to Eocene stiff clays. *Géotechnique* **67**, No. 8, 653–671, https://doi.org/10.1680/jgeot.15.P.227.

Cafaro, F. & Cotecchia, F. (2001). Structure degradation and changes in the mechanical behaviour of a stiff clay due to weathering. *Géotechnique* **51**, No. 5, 441–453, https://doi.org/10.1680/geot.2001.51.5.441.

Chandler, R., Leroueil, S. & Trenter, N. (1990). Measurements of the permeability of London Clay using a self-boring permeameter. *Géotechnique* **40**, No. 1, 113–124, https://doi.org/10.1680/geot.1990.40.1.113.

Cotecchia, F. (2003). Mechanical behaviour of the stiff clays from the Montemesola Basin in relation to their geological history and structure. In *Proceedings of international symposium on characterisation and engineering properties of natural soils* (eds T. S. Tan, K. K. Phoon, D. W. Hight and S. Leroueil), vol. 2, pp. 817–850. Lisse, the Netherlands: A. A. Balkema.

Cotecchia, F. & Chandler, R. J. (1995). The geotechnical properties of the Pleistocene clays of the Pappadai valley. *Q. J. Engng Geol.* **28**, No. 1, 5–22.

Dao, L. Q., Cui, Y. J., Tang, A. M., Pereira, J. M., Li, X. L. & Silen, X. (2014). Investigating the anisotropy of the shear modulus of natural Boom Clay. *Géotechnique Lett.* **4**, No. 2, 98–101, https://doi.org/10.1680/geolett.14.00015.

Delage, P. & Lefebvre, G. (1984). Study of the structure of a sensitive Champlain clay and its evolution during consolidation. *Can. Geotech. J.* **21**, No. 1, 21–35.

Griffiths, F. J. & Joshi, R. C. (1990). Clay fabric response to consolidation. *Appl. Clay Sci.* **5**, No. 1, 37–66.

Guglielmi, S., Cotecchia, F., Cafaro, F. & Gens, A. (2022). Analysis of the micro to macro response of clays to compression. *Géotechnique*, https://doi.org/10.1680/jgeot.21.00233.

Lapierre, C., Leroueil, S. & Locat, J. (1990). Mercury intrusion and permeability of Louiseville clay. *Can. Geotech. J.* **27**, No. 6, 761–773.

Leroueil, S., Bouclin, G., Tavenas, F., Bergeron, L. & La Rochelle, P. (1990). Permeability anisotropy of natural clays as a function of strain. *Can. Geotech. J.* **27**, No. 5, 568–579.

Leroueil, S., Hamouche, K., Tavenas, F., Boudali, M., Locat, J., Virely, D., Roy, M., La Rochelle, P. & Leblond, P. (2003). Geotechnical characterisation and properties of a sensitive clay from Quebec. In *Proceedings of international symposium on characterisation and engineering properties of natural soils* (eds T. S. Tan, K. K. Phoon, D. W. Hight and S. Leroueil), vol. 1, pp. 363–394. Lisse, the Netherlands: A. A. Balkema.

Locat, J. (1995). On the development of microstructure in collapsible soils: lessons from the study of recent sediments and artificial cementation. In *Genesis and properties of collapsible soils* (eds E. Derbyshire, T. Dijkstra and I. J. Smalley), NATO ASI Series C: Mathematical and Physical Sciences, vol. 468, pp. 93–128. Amsterdam, the Netherlands: Kluwer Academic (Springer Science + Business Media).

Locat, J. & Tanaka, H. (2001). A new class of soil: fossilifereous soils? In *Proceedings of the 15th international conference on soil mechanics and geotechnical engineering*, vol. 3, pp. 2295–2300. Lisse, the Netherlands: A. A. Balkema.

Lollino, P., Cotecchia, F., Zdravkovic, L. & Potts, D. M. (2005). Numerical analysis and monitoring of Pappadai dam. *Can. Geotech. J.* **42**, No. 6, 1631–1643.

Lumb, P. & Holt, J. K. (1968). The undrained shear strength of a soft marine clay from Hong Kong. *Géotechnique* **18**, No. 1, 25–36, https://doi.org/10.1680/geot.1968.18.1.25.

O'Brien, N. R. & Slatt, R. M. (1990). *Argillaceous rock atlas*. Berlin, Germany: Springer-Verlag.

Sfondrini, G. (1975). Caratteristiche microtessiturali e microstrutturali di alcuni sedimenti argillosi connesse con la natura ed il tipo delle sollecitazioni subite. *Geol. Appl. Idrogeol.* **10**, 300–320 (in Italian).

Skempton, A. W. (1969). The consolidation of clays by gravitational compaction. *Q. J. Geol. Soc.* **125**, 373–411.

Skempton, A. W. & Northey, R. D. (1952). The sensitivity of clays. *Géotechnique* **3**, No. 1, 30–53, https://doi.org/10.1680/geot.1952.3.1.30.

Soccodato, F. M. (2003). Geotechnical properties of Fucino clayey soil. In *Proceedings of international symposium on characterisation and engineering properties of natural soils* (eds T. S. Tan, K. K. Phoon, D. W. Hight and S. Leroueil), vol. 1, pp. 791–807. Lisse, the Netherlands: A. A. Balkema.